Table 2-1 The conditions of H_2, NH_3, and O_2 plasma treatments for Methylsilsesquiazane (MSZ)

Gas	Time (min)	Flow rate (sccm)	Pressure (mtorr)	Power (W)	Temperature (°C)
H_2	3	400	500	100	250
	6				
	9				
NH_3	3	700	300	200	300
	6				
	9				
O_2	3	900	650	110	250
	6				
	9				

Table 2-2 The parameters of CMP process

Polisher: ***IPEC372M***	**1st Step (only)**		
	Phase 1	Phase 2	
Platen/ Carrier Speed	50/60 rpm	30/40 rpm	
Down Force	3.0 psi	1.5 psi	
Back Pressure	2.0 psi	0	
Slurry Flow Rate	150 ml/cm	Rinse	
Time	2 min	30 sec	
Polishing Pad	Rodel Politex Regular E. ™		
Carrier Film	Rodel R200-T3 ™		
Slurry Formation	SS-25 Slurry	Cu-Slurry	TaN-Slurry
	SS-25 slurry : DI water: TMAH =14:14:5 (vol%)	2 vol% HNO_3, 5×10^{-2} M Citric acid, 3 wt% Al_2O_3(0.1μm)	10 wt% Colloidal silica, 10 vol% H_2O_2, pH=8.5

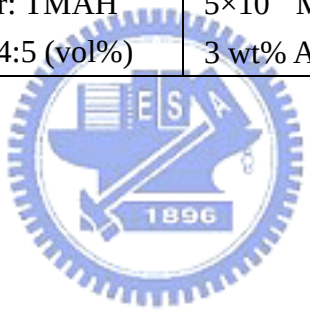

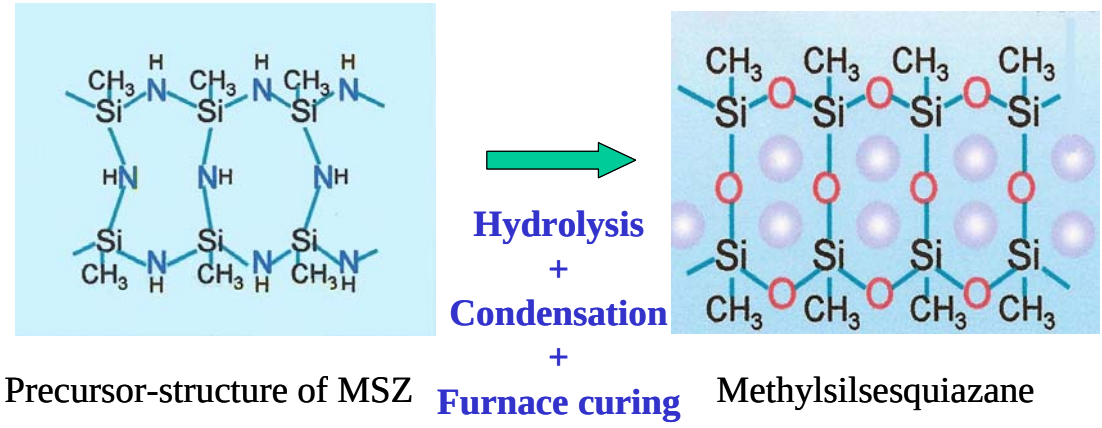

Figure 2-1 Formation mechanism of MSZ film.

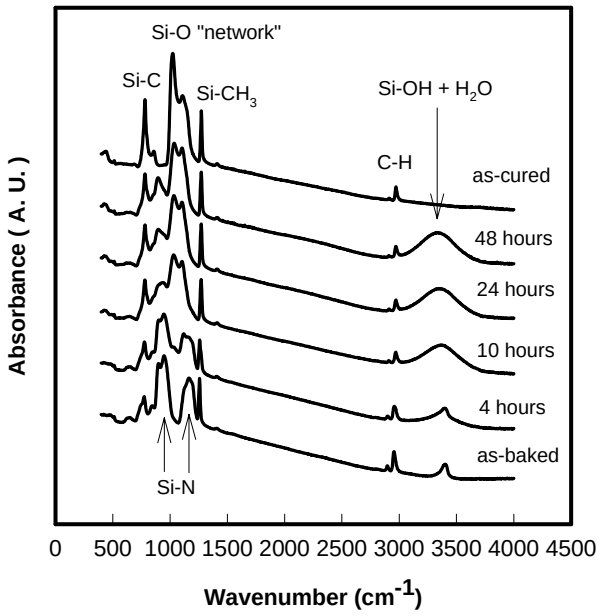

Figure 2-2 FTIR spectra of MSZ film during formation.

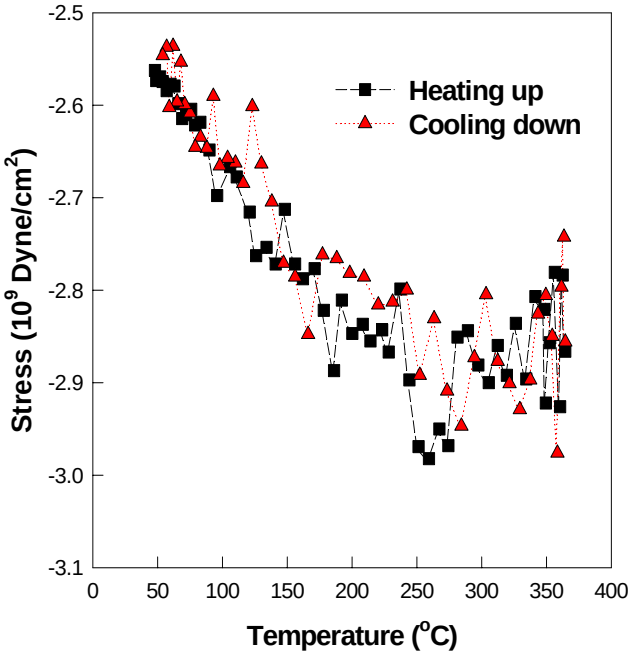

Figure 2-3 The internal stress variation of MSZ film during thermal cycle.

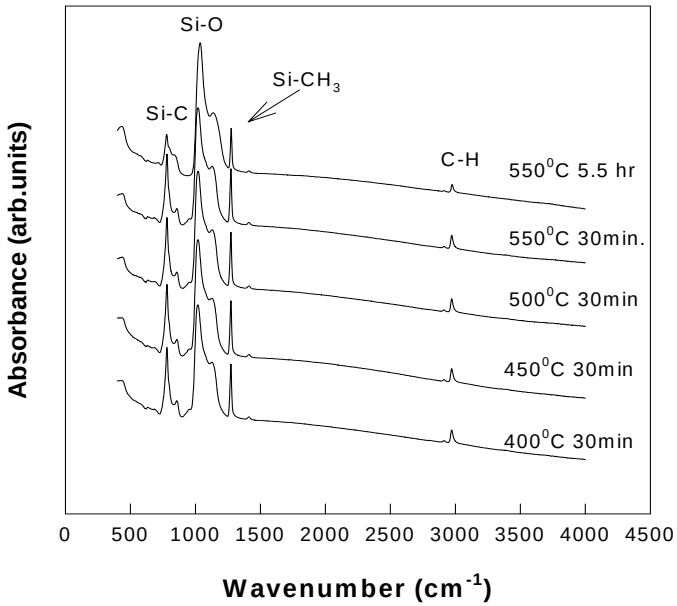

Figure 2-4 FTIR spectra of MSZ films after various anneal temperature.

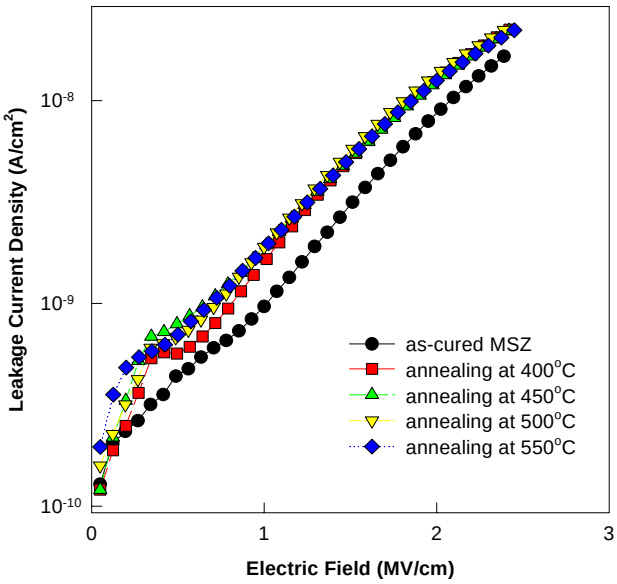

(a)

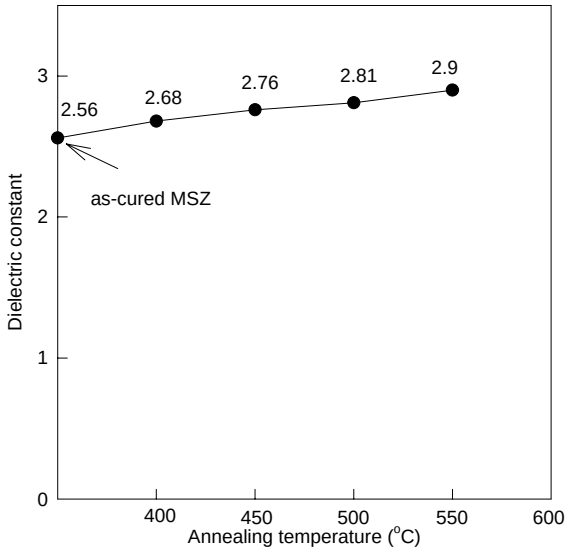

(b)

Figure 2-5 Dielectric properties of the MSZ film after thermal annealed at various temperature. **(a)** Leakage current density of the MSZ film versus electric field. **(b)** Dielectric constant of the MSZ film versus annealing temperature.

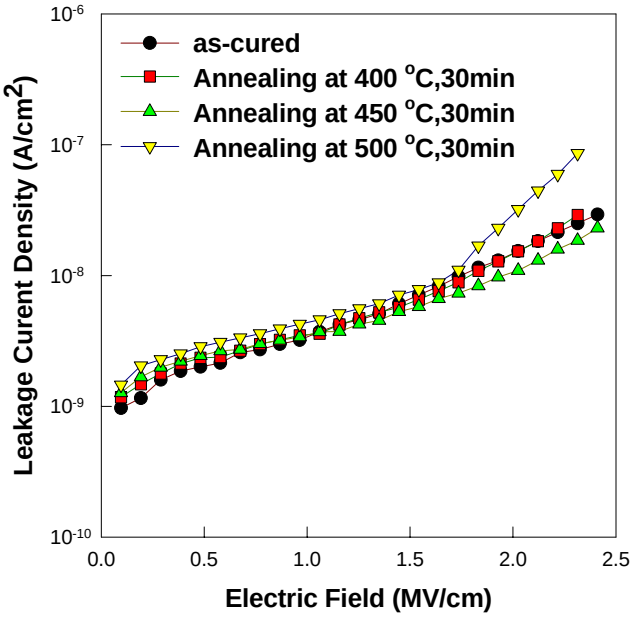

(a)

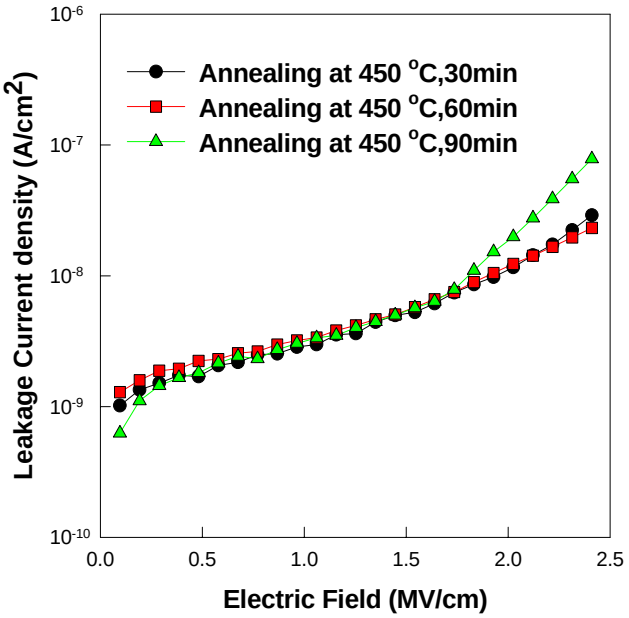

(b)

Figure 2-6 The leakage current density of (a) temperature and (b) time dependence of thermal stress for Cu electrode MIS structure.

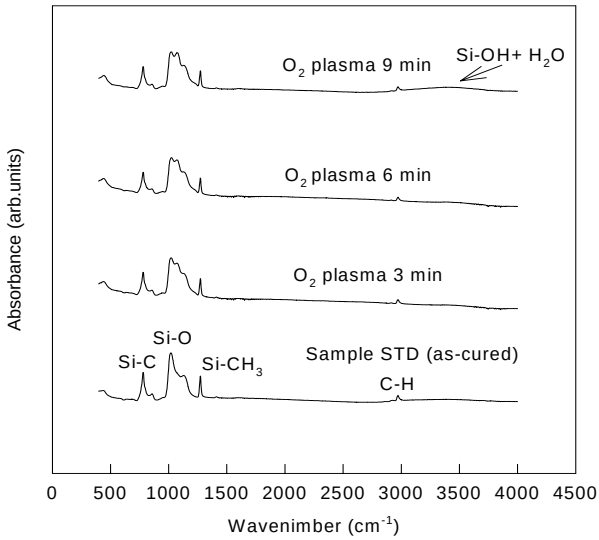

Figure 2-7 FTIR spectra of MSZ film after O_2 plasma treatment for 3 to 9 minutes

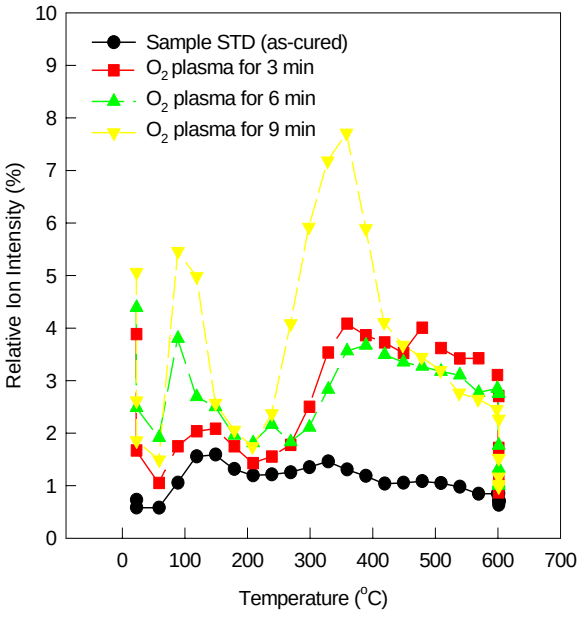

Figure 2-8 The TDS moisture desorption spectra of O_2 plasma-treated MSZ films.

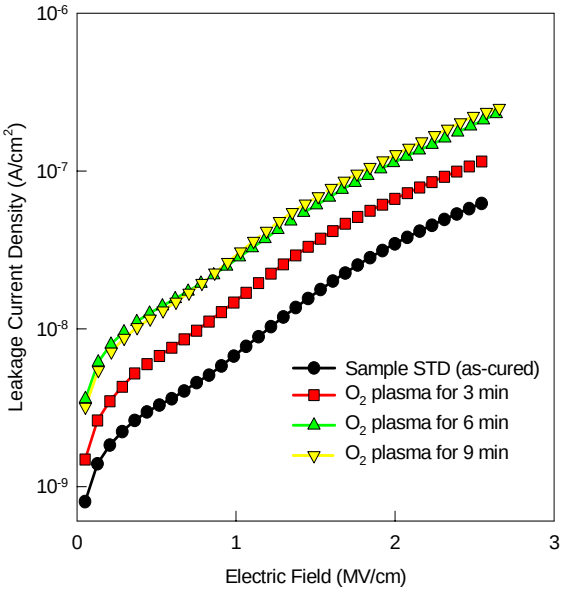

(a)

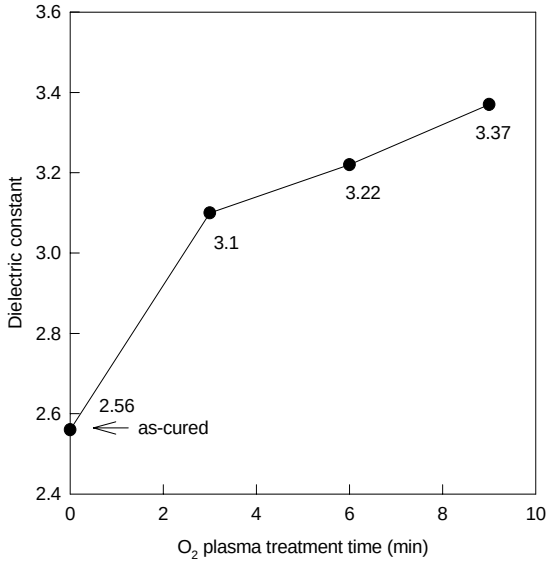

(b)

Figure 2-9 Dielectric properties of MSZ after O_2 plasma treatment. **(a)** Leakage current density of the MSZ versus electric field. **(b)** Dielectric constant of the MSZ versus O_2 plasma treatment time.

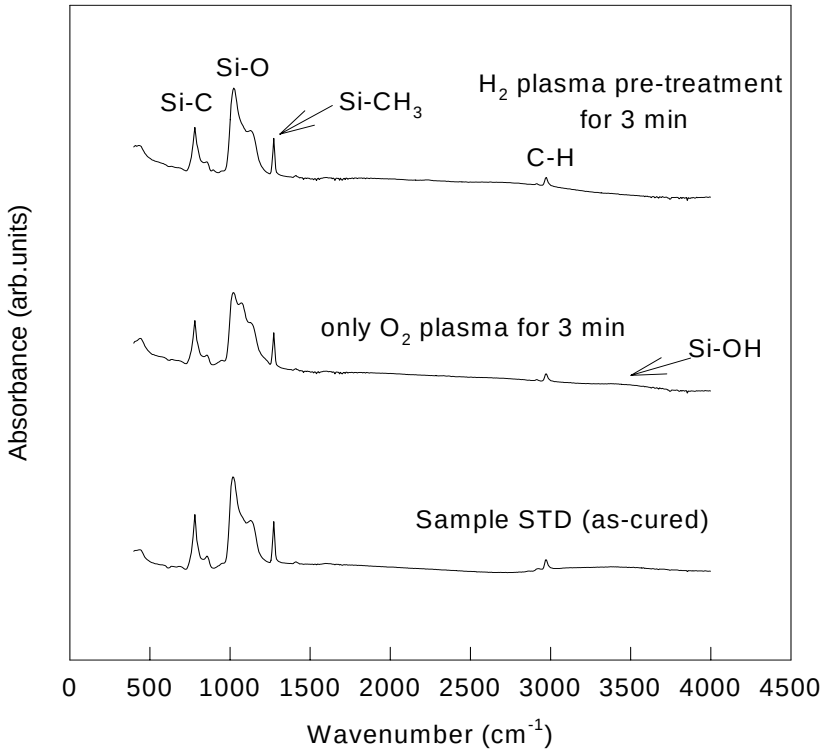

Figure 2-10 FTIR spectra of as-cured and H_2 plasma-treated 3 min films after undergoing O_2 plasma treatment..

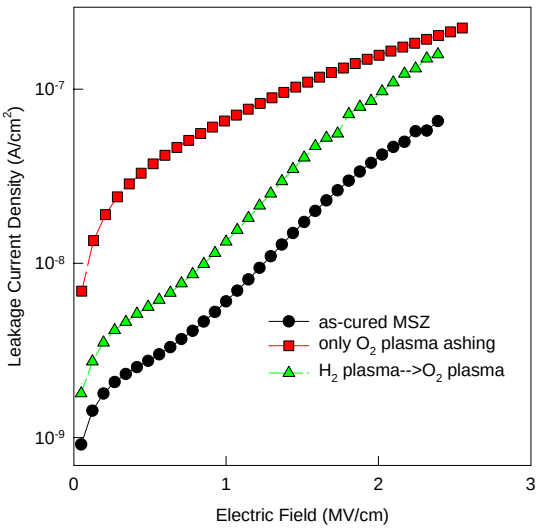

(a)

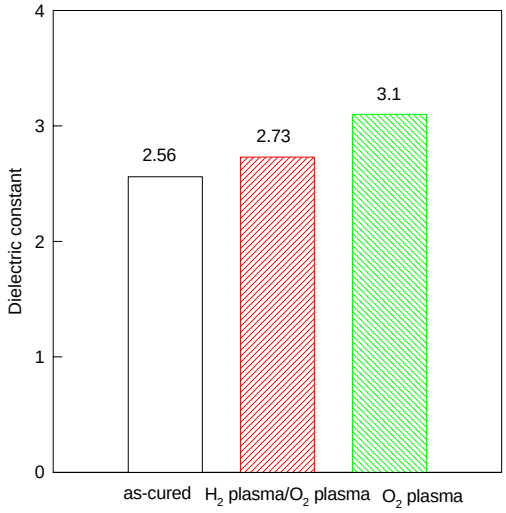

(b)

Figure 2-11 Dielectric properties of as-cured and H_2 plasma-treated 3 min MSZ film after undergoing O_2 plasma exposure. **(a)** Leakage current density of the MSZ versus electric field. **(b)** Dielectric constant of the MSZ .

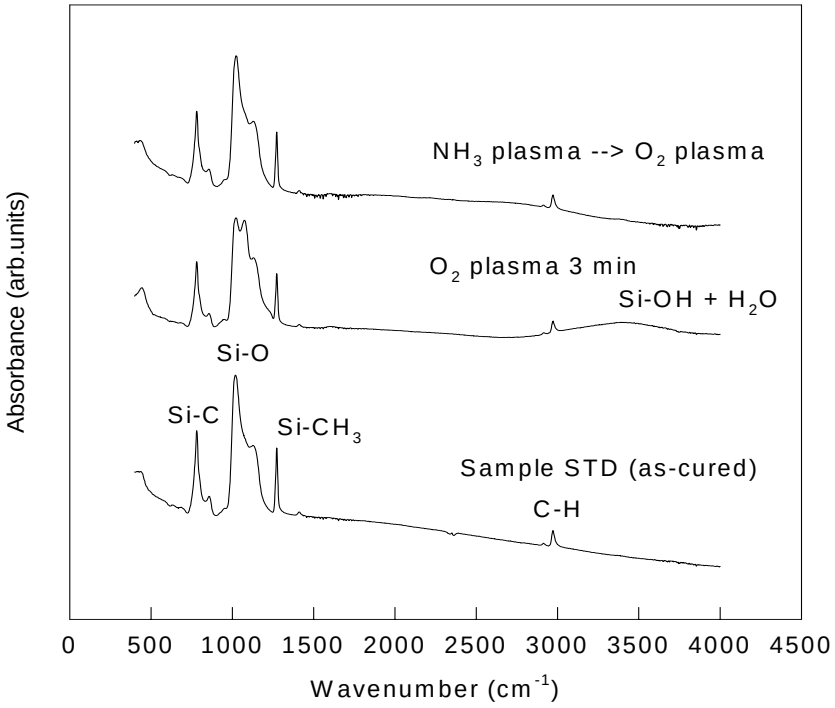

Figure 2-12 FTIR spectra of as-cured and NH_3 plasma-treated 3 min films after undergoing O_2 plasma treatment.

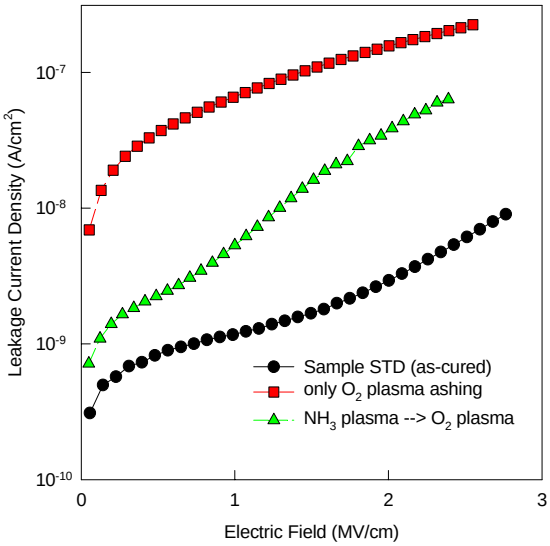

(a)

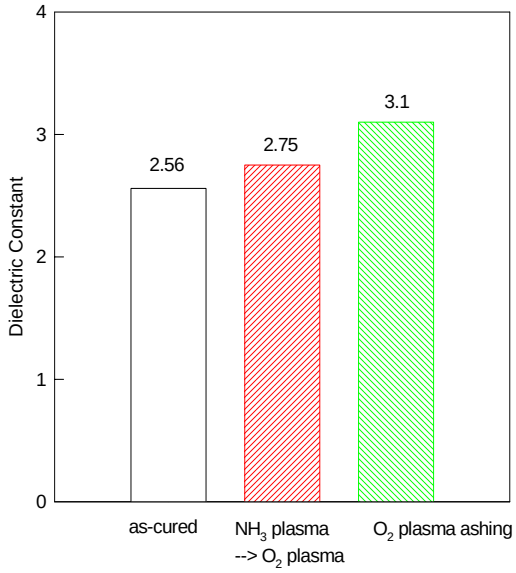

(b)

Figure 2-13 Dielectric properties of as-cured and NH_3 plasma-treated 3 min MSZ film after subjected to O_2 plasma exposure. **(a)** Leakage current density of the MSZ versus electric field. **(b)** Dielectric constant of the MSZ.

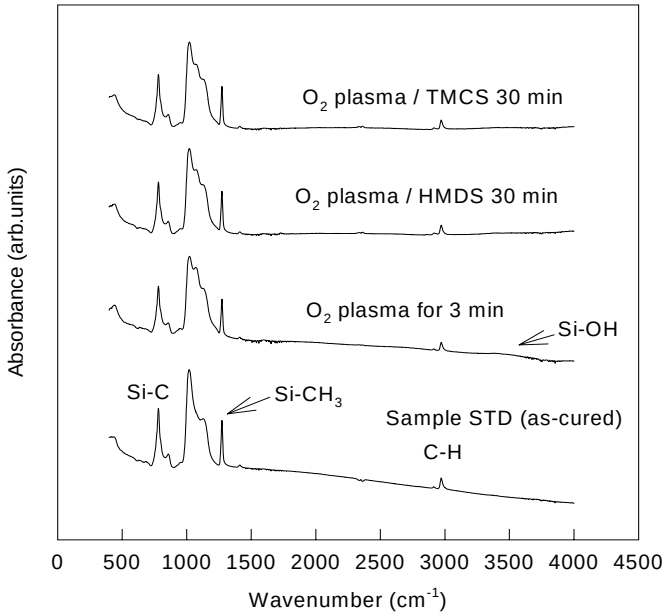

Figure 2-14 FTIR spectra of MSZ films with O_2 plasma and subsequent TMCS/HMDS treatment.

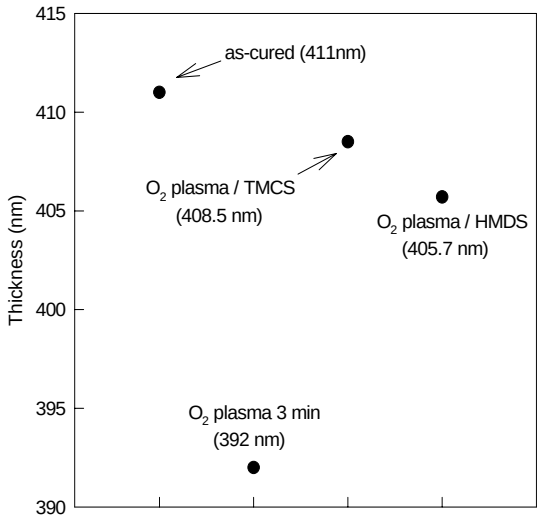

Figure 2-15 Thickness variation of MSZ films with O_2 plasma and subsequent TMCS/HMDS treatment.

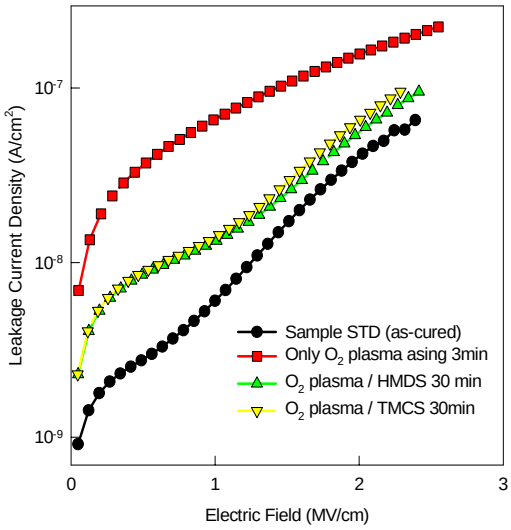

(a)

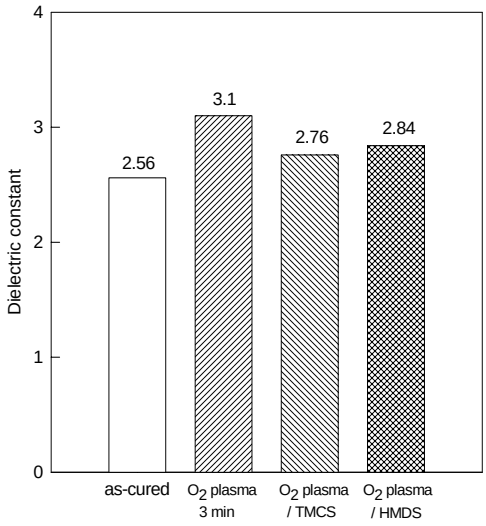

(b)

Figure 2-16 Dielectric properties of MSZ films with O_2 plasma and subsequent TMCS/HMDS treatment (a) leakage current density of the MSZ versus electric field (b) dielectric constant of the MSZ.

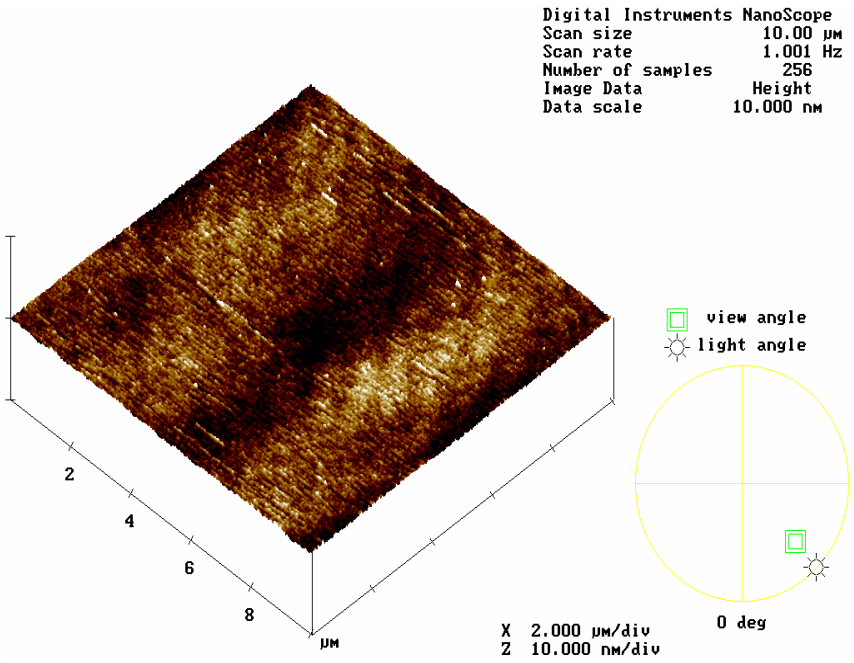

(a)

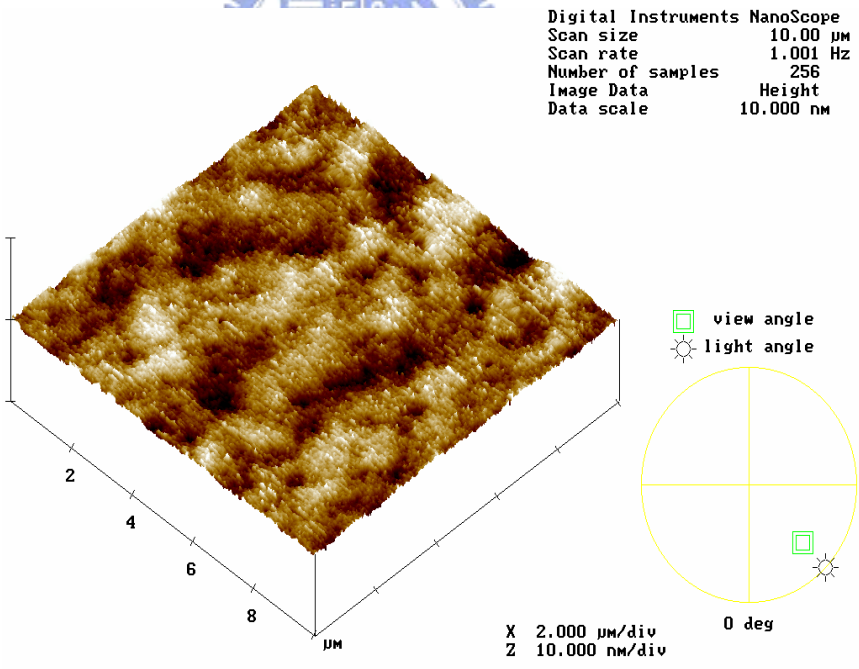

(b)

Figure 2-17 AFM image surface of polished MSZ (a) with TaN slurry (b) with Cu slurry.

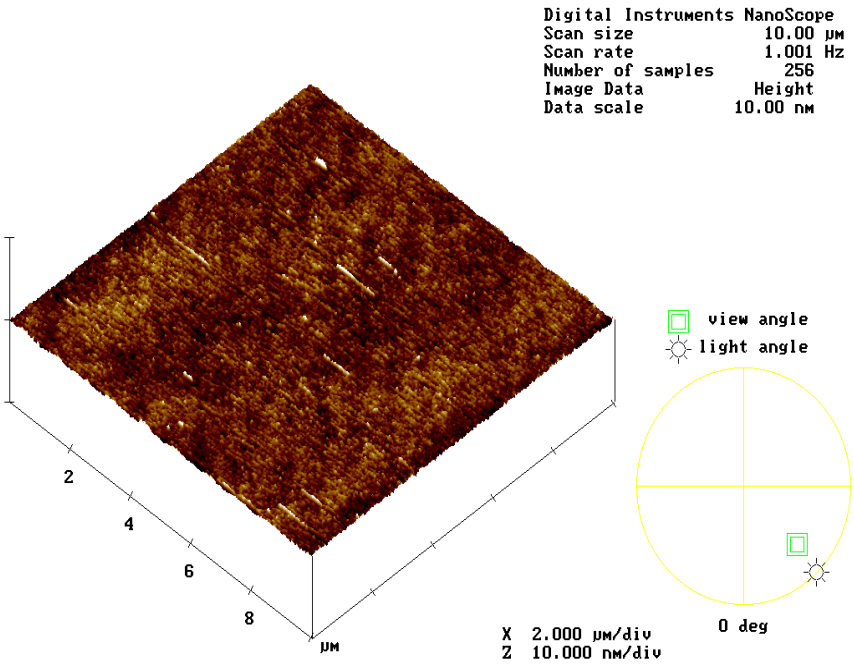

Figure 2-18 AFM micrograph surface of polished MSZ with commercial SS-25 slurry.

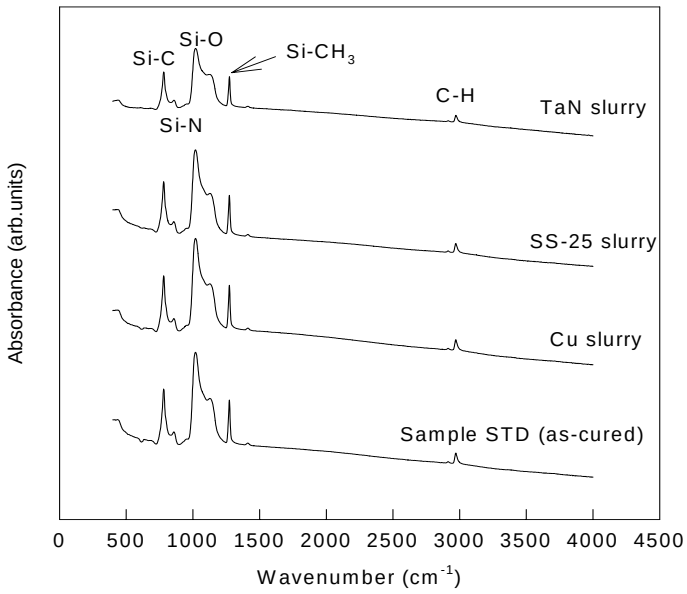

Figure 2-19 FTIR Spectra of post-CMP MSZ with various slurries.

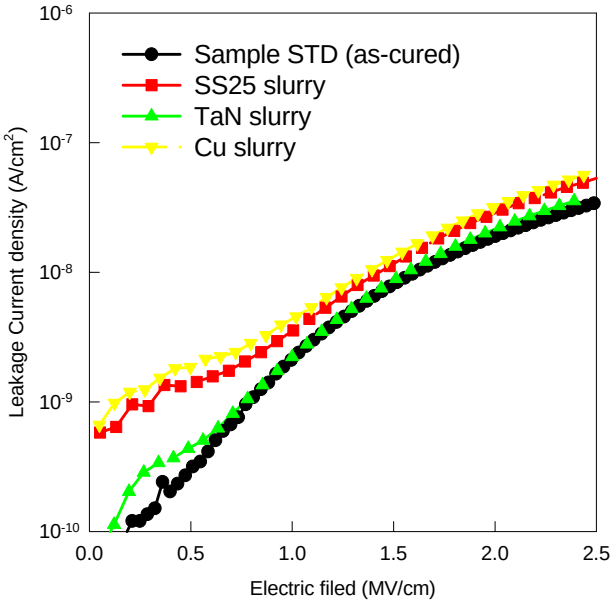

(a)

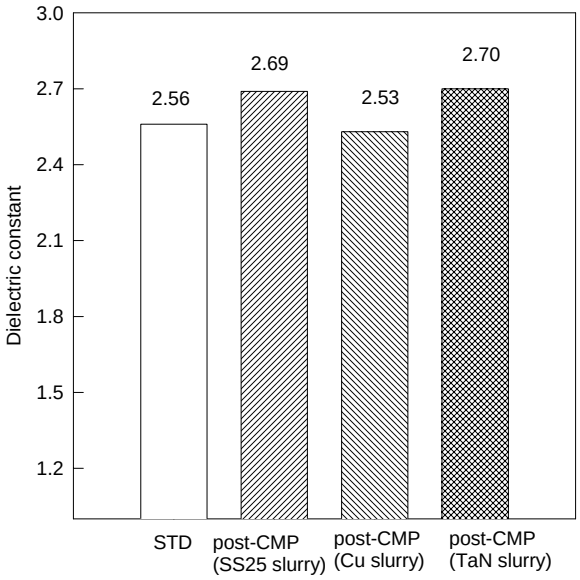

(b)

Figure 2-20 Dielectric properties of polished MSZ with various slurries. (a) leakage current density of post-CMP MSZ versus electric field (b) dielectric constant of post-CMP MSZ films.

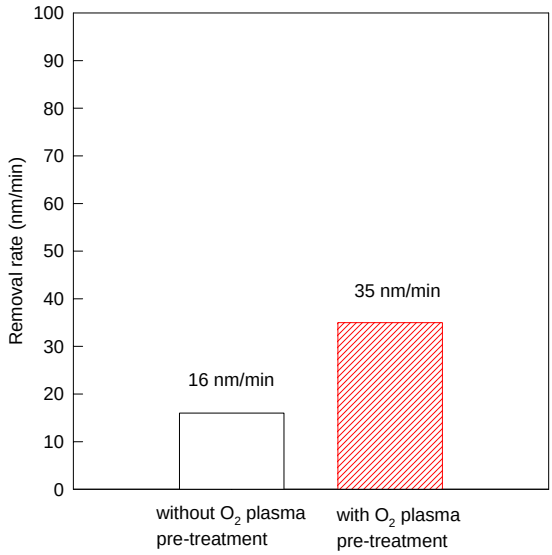

Figure 2-21 Removal rate of CMP for MSZ polished by SS-25 slurry with and without O_2 plasma pre-treatment

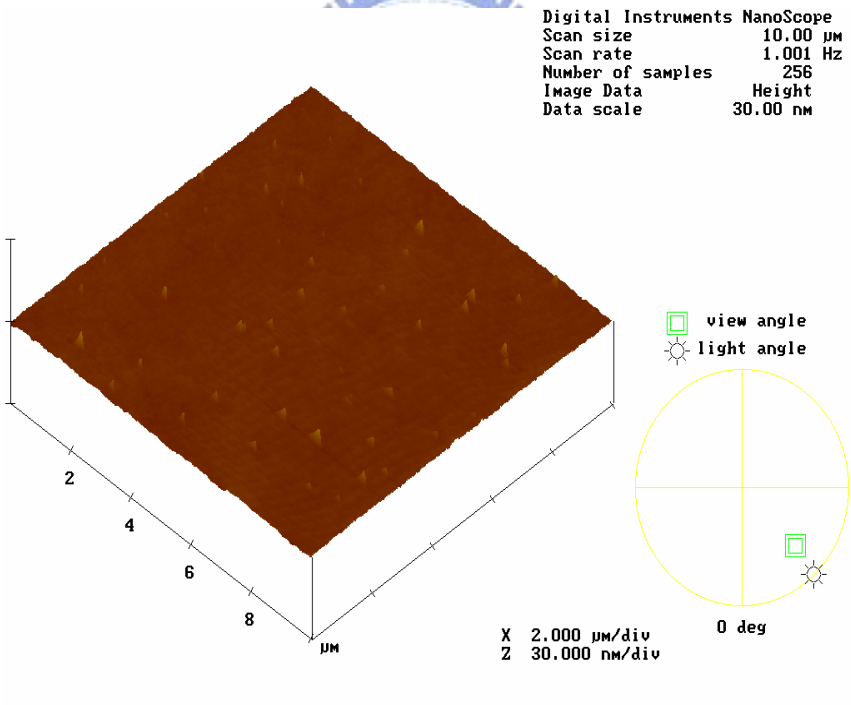

(a)

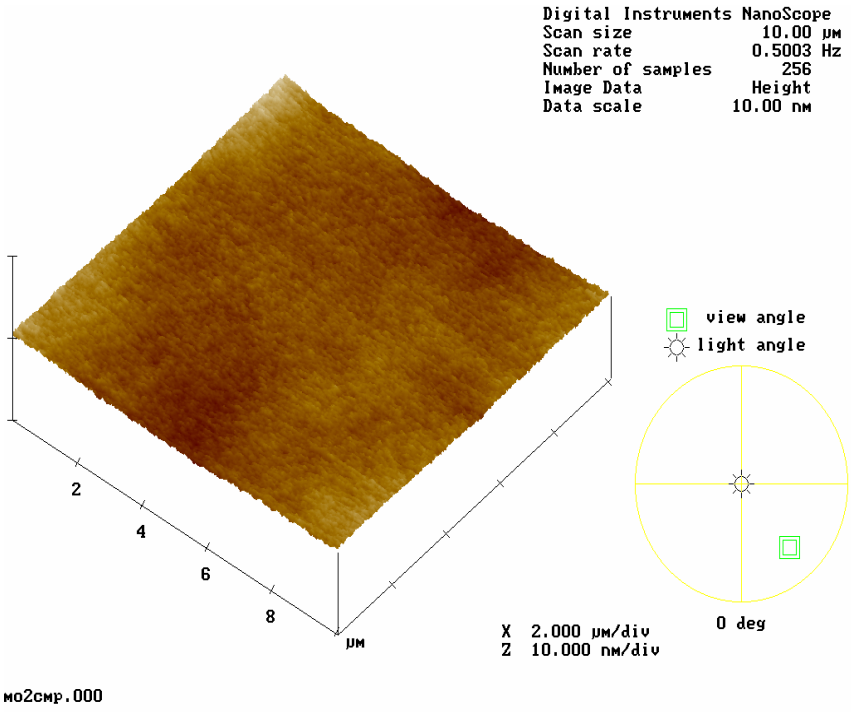

(b)

Figure 2-22 AFM micrographs of 1 min O_2 plasma-treated MSZ films (a) without CMP process (b) with CMP process.

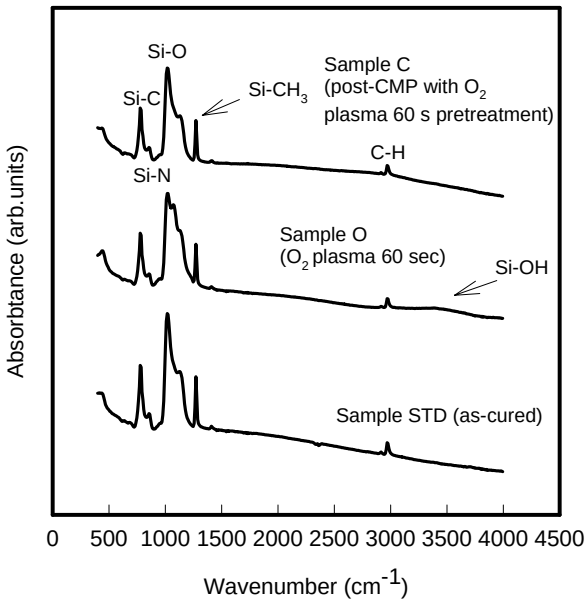

Figure 2-23 FTIR spectra of O_2 plasma-treated MSZ films before and after CMP process.

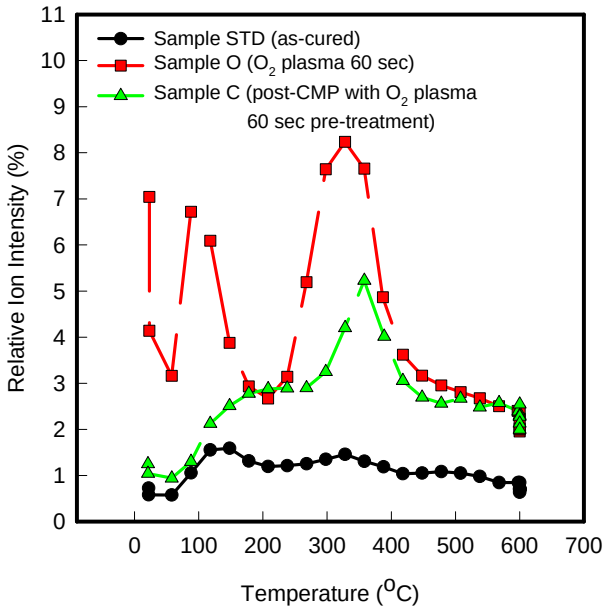

Figure 2-24 Moisture-desorption spectra of O_2 plasma-treated MSZ films before and after CMP process.

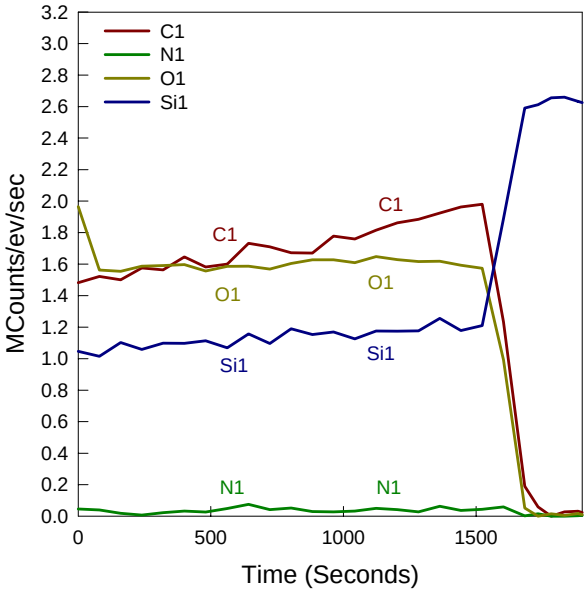

(a)

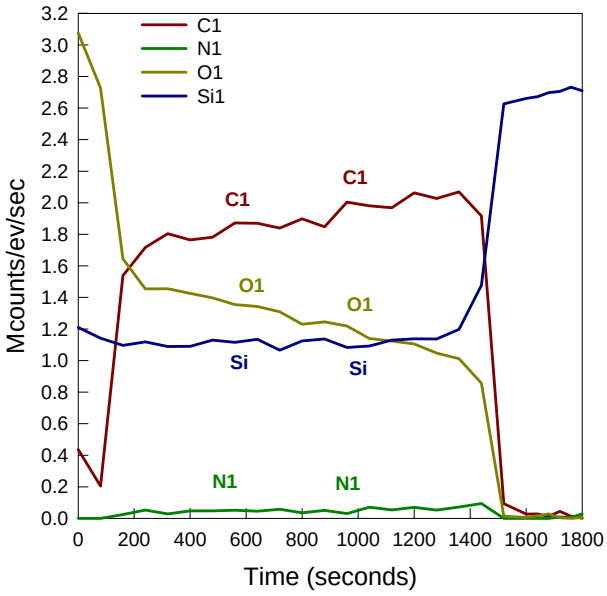

(b)

Figure 2-25 The auger depth profile of (a) as-cured and (b) 1 min O_2 plasma treated MSZ films.

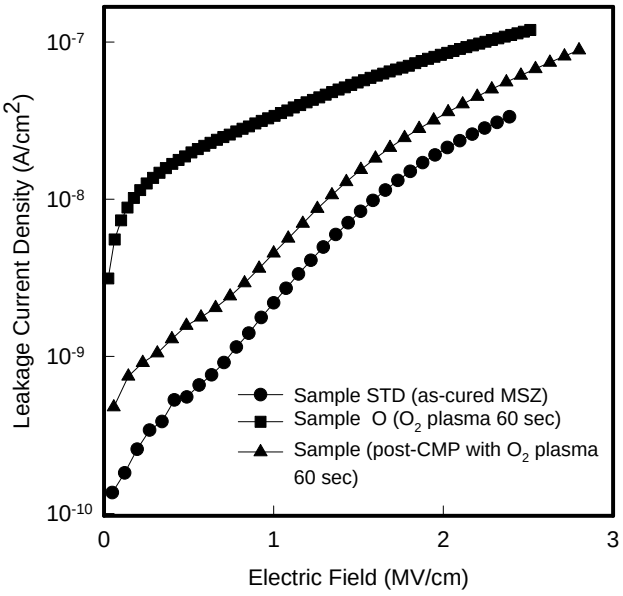

(a)

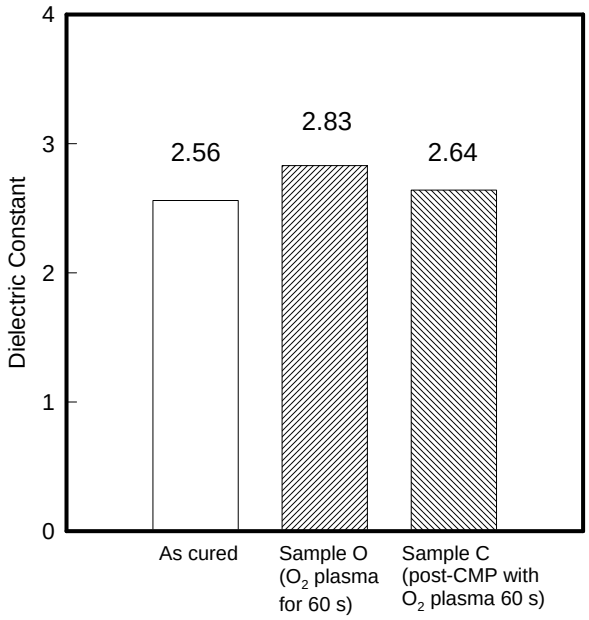

(b)

Figure 2-26 Dielectric properties of O_2 plasma-treated MSZ before and after CMP process (a) leakage current density of MSZ films as a function of electric field (b) variation in dielectric constant of O_2 plasma-treated MSZ films.

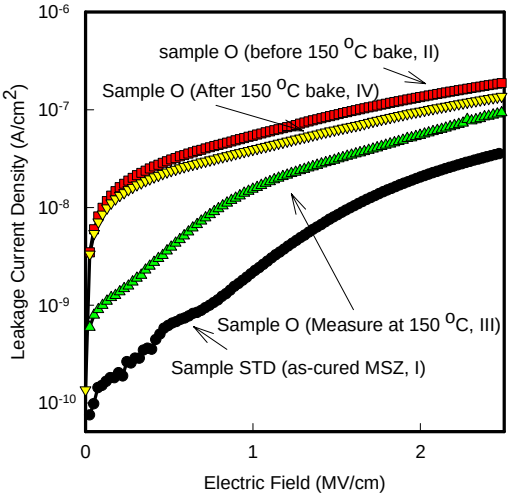

Figure 2-27 Leakage-current density of sample O before and after the 150 ^{o}C bake [curve I, sample STD measured at 25 ^{o}C; curve II, sample O measured at 25 ^{o}C (before 150 oC bake); curve III, sample O measured at 150 ^{o}C; curve IV, sample O measured at 25 ^{o}C (after 150 ^{o}C bake)].

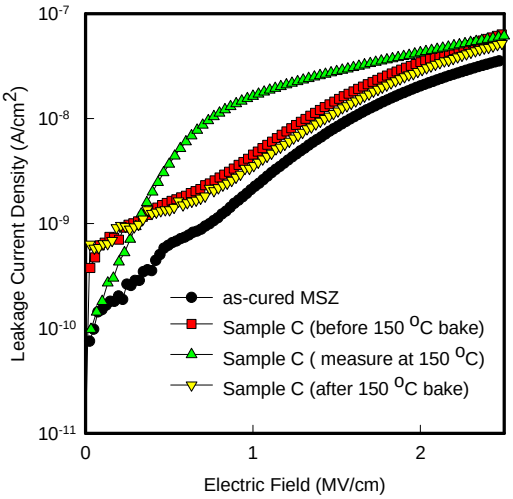

Figure 2-28 Leakage-current density of sample C before and after 150 ^{o}C bake [curve I, sample STD measured at 25 ^{o}C; curve II, sample C measured at 25 ^{o}C (before 150 ^{o}C bake); curve III, sample C measure at 150 ^{o}C; curve IV, sample C measured at 25 ^{o}C (after 150 ^{o}C bake)].